Preparation of Gold–Poly(vinyl pyrrolidone) Core–Shell Nanocomposites and Their Humidity-Sensing Properties

Xue Jiao Chen, Jian Zhang, Dian Fei Ma, Shi Chao Hui, Yan Li Liu, Wei Yao

Key Laboratory of Polar Materials and Devices, Ministry of Education, Department of Electrical Engineering, East China Normal University, Shanghai 200241, China

Received 15 September 2010; accepted 11 November 2010
DOI 10.1002/app.33751
Published online 4 March 2011 in Wiley Online Library (wileyonlinelibrary.com).

ABSTRACT: The humidity-sensing properties of gold (Au)–poly(vinyl pyrrolidone) (PVP) core–shell nanocomposites were investigated. Au–PVP nanocomposites were synthesized and then incorporated into a capacitive-type humidity sensor as a dielectric. Because of the adsorption/desorption of water molecules, the variation of capacitance under different humidity levels was examined by the capacitance–frequency conversion circuit and recorded by a LabVIEW system in terms of the frequency shift. As the relative humidity (RH) increased from 11.3 to 93%, the output frequency decreased monotonically, with a sen sitivity of about −136 Hz/% RH. Also, the good reproducibility and stability, fast response, and low hysteresis made the pellet a suitable candidate for humidity sensing. © 2011 Wiley Periodicals, Inc. J Appl Polym Sci 121: 1685–1690, 2011

Key words: core–shell polymers; nanocomposites; nanotechnology

INTRODUCTION

In recent years, there has been increasing interest in core–shell composite structures, as they can play a vital role in determining a material's properties. So far, many core–shell hybrid structures have been successfully achieved, such as gold Au–AgCl-polyaniline for glucose biosensors,[1] Cu-Au for DNA detection,[2] Au–SiO_2 for single electron transistors,[3] ZnO–Y_2O_3,[4] NiO/Al_2O_3[5] for humidity sensors, and poly(methyl methacrylate)–phosphor composites for application in poly(vinyl chloride) matrixes.[6]

In recent studies, Au nanoparticles have received special attention in various fields, such as biosensors and chemical sensors. This is due to their special characteristics, including high thermal and electrical conductivities, high corrosion, and oxidation resistance, even in the nanometer-size region.[7] In addition, they offer a unique surface chemistry that allows them to be used as platforms on which layers of organic molecules self-assemble.[8]

Compared with Au nanoparticles, polymer-coated Au nanoparticles exhibit some improved properties, such as better stability and linearity, which give them potential as humidity-sensing materials.[9] In our study, the coating of poly(vinyl pyrrolidone) (PVP) with Au was one such approach, and one of our objectives was to improve the humidity-sensing performance. PVP thin films, as humidity-sensing materials, usually suffer from a small surface-to- volume ratio and high intrinsic electrical impedance. If PVP-encapsulated Au nanocomposites were used to replace original PVP thin films, the enlarged surface-to-volume ratio and the improved conductivity would probably improve the humidity-sensing performance, for example, by giving the films a higher sensitivity. Water adsorption/desorption benefits from the submicron thickness of PVP cladding on Au nanoparticles.

In this study, desired Au–PVP core–shell nanocomposites, as shown in Figure 1, were prepared. Their surface morphology and structures were characterized. Finally, this kind of nanocomposite was introduced into the gap of the electrode pairs to act as dielectrics of the capacitive-type humidity sensor. The humidity-sensitive characteristics of the developed nanocomposites were investigated carefully by our homemade capacitance–frequency conversion circuit.

EXPERIMENTAL

Raw materials

PVP, chloroauric acid, and trisodium citrate were commercially available from Sinopharm Chemical Reagent Co., Ltd. (Shanghai, China). They were all

Correspondence to: J. Zhang (jzhang@ee.ecnu.edu.cn).
Contract grant sponsor: National Natural Science Foundation of China; contract grant numbers: 60672002, 61076070.
Contract grant sponsor: Innovation Program of Shanghai Municipal Education Commission; contract grant number: 09ZZ46.

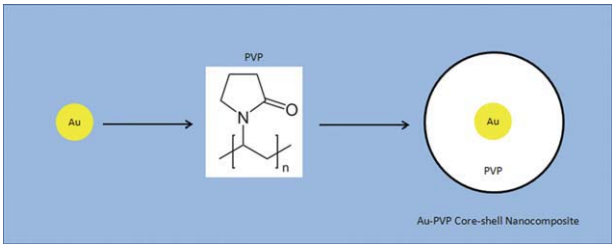

Figure 1 Schematic structure of the prepared Au–PVP core–shell nanocomposite. [Color figure can be viewed in the online issue, which is available at wileyonlinelibrary.com.]

analytical reagents and were used without further purification. Deionized water (18 MΩ), purified with an ultrapure deionized water system, was used for all experiments.

Preparation of the Au–PVP core–shell nanocomposites

In this study, the first step was to prepare dispersed Au nanoparticles in an aqueous solution by the citrate reduction of $HAuCl_4$.[10,11] Trisodium citrate solution (300 mL, 38.8 m*M*) was added to 30 mL of a rapidly boiling $HAuCl_4$ solution (1 m*M*), and the dispersed Au nanoparticles in the aqueous solution were prepared after 10 min, when the color of the solution changed from pale yellow to dark red. The diameter of the as-achieved Au nanoparticles was around 10 nm.[12,13] Second, the PVP solution (3.0 g/dL) was prepared at 70°C and mixed with the well-distributed Au-nanoparticle-containing solution for 5 h of stirring. After the second step, the mixture was filtered and kept still for about 30 h at room temperature for aging. The diameter of the as-synthesized Au–PVP core–shell nanocomposites could reach several hundred namometers.[14] The as-received Au–PVP core–shell structure is as shown in Figure 1.

Humidity-sensing mechanism

The testing circuit is shown in Figure 2, where a silicon chip was used as the substrate and silver paste was used to construct a pair of electrodes on the substrate. The Au–PVP nanocomposites were incorporated into the gap of the electrodes to simultaneously act as dielectrics and as the adsorbent for the capacitive humidity sensor. The effective dielectric constant (ε_{eff}) can be expressed as[15]

$$\varepsilon_{eff} = \varepsilon_{adsorbent} + V(\varepsilon_{absorbate} - \varepsilon_{adsorbent})$$

where $\varepsilon_{adsorbent}$ is the dielectric constant of the Au–PVP core–shell nanocomposites, $\varepsilon_{absorbate}$ is the dielectric constant of water in this study, and V is the volume fraction of condensed adsorbate in the adsorbent, which is related to the relative humidity (RH) value. The dielectric constant of the nanocomposites was low, about 5, compared with the one of water (~80).[16,17] Hence, under different humidity environments, the dielectric constant was different because of the water uptake, and it finally led to a big variation in capacitance.

Measurement system

To measure the nanocomposites' humidity characteristics, the measurement system was set up and is shown in Figure 3(a). The humidity-controlled environments (11.3, 23, 43, 57, 68, 75, 85, and 93% RH) were achieved with saturated aqueous solution of LiCl, CH_3COOK, K_2CO_3, NaBr, KI, NaCl, KCl, and KNO_3, respectively, at room temperature (~ 25°C).[18] Different humidity environments led to different effective dielectric constants, that is, different capacitances. The oscillation circuit could transfer the capacitance changes into frequency shifts. The output frequency was recorded by a homemade LabVIEW system.

The oscillating circuit is shown in detail in Figure 3(b), in which 555 time-base circuits were used to convert the capacitance changes into output frequency variations. In the testing process, the Au–PVP nanocomposites were incorporated into the capacitor component labeled *C* in Figure 3(b) for the 555 capacitance–frequency conversion circuits. According to the following equation, the capacitance variation due to the humidity environment correspondingly led to output frequency (*f*) changes, which were collected by the LabVIEW program in the computer:

$$f = \frac{1}{T} = \frac{1}{(R_1 + 2R_2)C\ln 2}$$

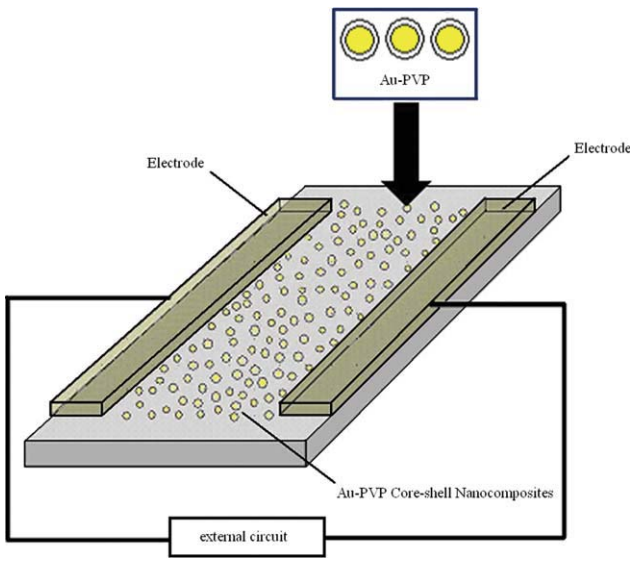

Figure 2 Humidity sensors' construction. [Color figure can be viewed in the online issue, which is available at wileyonlinelibrary.com.]

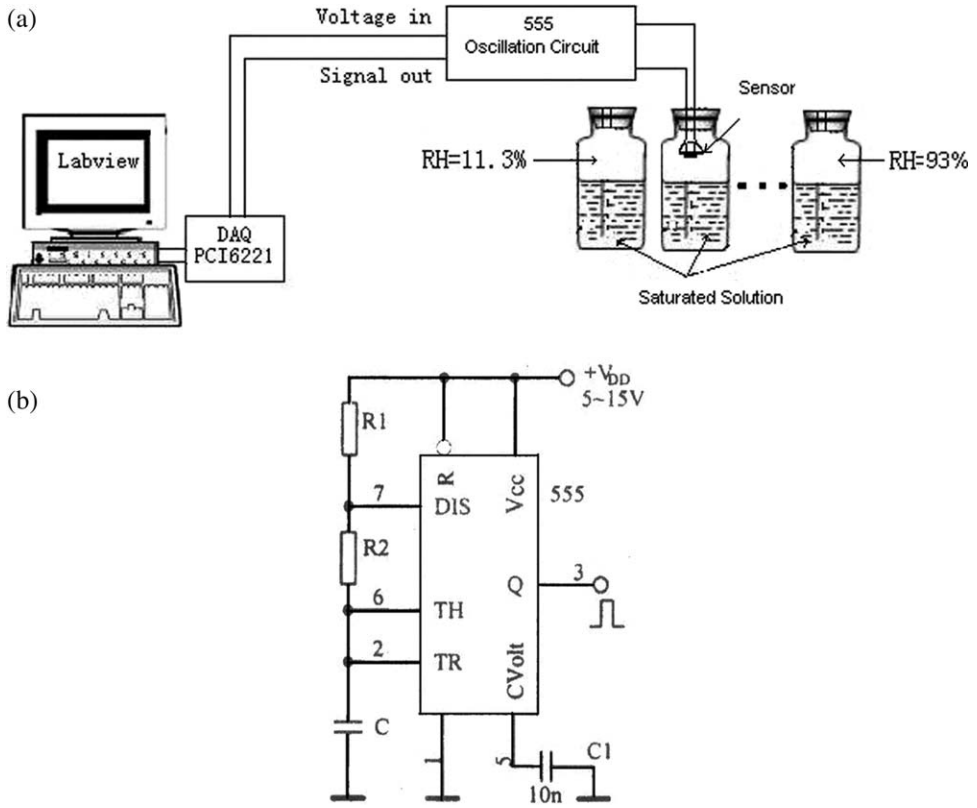

Figure 3 (a) Schematic diagram of the humidity measurement system. (b) Capacitance–frequency conversion circuit, where C is the humidity sensor. R1, R2 are resistors, R represents reset, DIS represents discharge, TH represents threshold, TR represents trigger, V_{CC} represents collector voltage, V_{DD} represents drain voltage, and Q represents output in digital circuits.

where T is the time, C is the capacitance, and R is the resistance. The entire setup was maintained at room temperature and in a clean environment.

RESULTS AND DISCUSSION

Characterization of Au–PVP core–shell nanocomposites

The as-obtained Au nanoparticles and as-synthesized Au–PVP nanocomposites were first examined by field emission scanning electron microscopy SEM; Hitachi S4700 (Tokyo, Japan) and SEM JSM-6360LA JEOL, (Tokyo, Japan). Both of them worked at room temperature and in a superclean environment. The images are shown in Figure 4(a,b), respectively. The average diameter of the Au nanoparticles was around 10 nm, which was in accordance with published results.[12,13] With PVP encapsulation, the Au–PVP core–shell nanocomposites' average diameter was about 780 nm, as shown in Figure 4(b), which was greatly larger than that of the Au nanoparticles; this indicated that the PVP was deposited onto the Au nanoparticles.

The surface morphology of the Au–PVP nanocomposites was examined by atomic force microscopy (AFM; VEECO Dimension 3100), which works at room temperature and in a superclean environment, and the images are shown in Figure 5. We observed that the nanocomposites dispersed uniformly with no formation of agglomerates.

Humidity-sensing properties measurement

In this study, the humidity-sensing properties of Au–PVP nanocomposites were tested under different RHs. The parameters, including humidity sensitivity, repeatability, stability, response time, and hysteresis properties, were evaluated.

The relationship between the shifted frequencies for the capacitive humidity sensor and RH is presented in Figure 6. As the RH level increased, the output frequency of the Au–PVP nanocomposites shifted monotonically to a lower frequency. In other words, negative frequency shifts were observed; this indicated that the adsorbed water led to an increased dielectric constant and increased the capacitance. When the RH level changed from 11.3 to 93% RH, the frequency shift reached around 12 kHz. The absolute deviations were also calculated and are shown in Figure 6 as its error range. Each data was measured five times. The results are shown in Figure 6.

Figure 6 also shows the linear fitting results, and the R^2 value was 0.9025, where R is the correlation

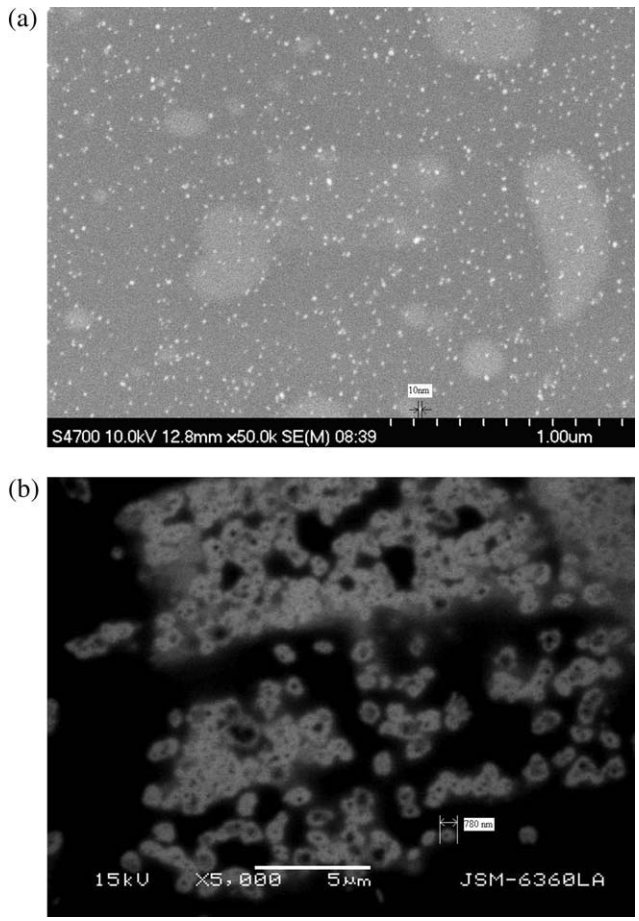

Figure 4 SEM images of the (a) Au nanoparticles and (b) Au–PVP nanocomposites.

coefficient. The sensitivity value was defined as the slope of the fitting curve (Hz/% RH in Fig. 6). It was about −136 Hz/% RH for the Au–PVP nanocomposites, which indicated that the Au–PVP nanocomposites had a high humidity sensitivity and good linearity.

To study the humidity repeatability, the nanocomposites were put into two fixed-humidity-level environments repeatedly, and the output frequency values were recorded. The sensor responses under two fixed humidity conditions, which corresponded to 11.3–43–11.3% RH and 11.3–85–11.3% RH, respectively, were tested, and the results are shown in Figure 7(a,b). As shown in the figure, the output frequencies were nearly reversible or repeatable when the nanocomposites was submitted to humidity cycling. For example, for 11.3–85–11.3% RH cycling, the output frequency changed from about 36,700 Hz (at 11.3% RH) to 28,000 Hz (at 43% RH) and then about 36,400 Hz (back to 11.3% RH), which was very close to the initial value of the cycle. The result indicates that the Au–PVP nanocomposite had good repeatability and good response behavior for humidity sensing.

Stability is an important parameter of humidity-sensing properties. The short-term stability of the nanocomposites, which was about 3.4 h, was studied under a fixed humidity level. The results under 85% RH are shown in Figure 8. The output frequency value of the Au–PVP nanocomposites fluctuated slightly, along with the time and maximum fluctuation rate ($|f - f_{average}|/f_{average} \times 100\%$) was only around 2.2%, which indicated that the nanocomposites performed well on stability.

Several tests under different humidity levels indicated that, generally, the humidity sensor response could reach stability within 10 min. Therefore, the test period was set to this value, which was similar to the one reported in ref. 19. In our study, the response time was defined as the 0–63% value from total time taken by the nanocomposites for a change

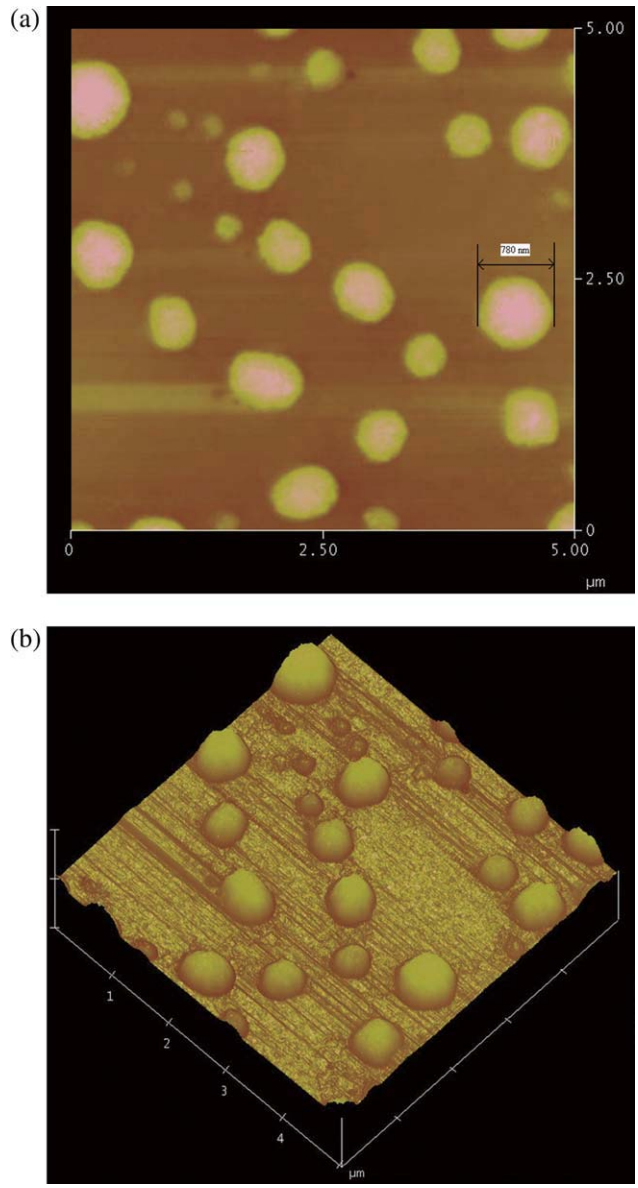

Figure 5 AFM images of the Au–PVP nanocomposites. [Color figure can be viewed in the online issue, which is available at wileyonlinelibrary.com.]

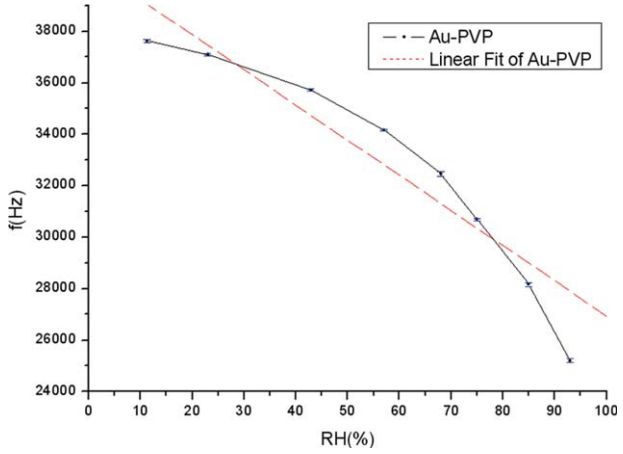

Figure 6 Relationship between the shifted frequencies for the Au–PVP nanocomposites and the RH. [Color figure can be viewed in the online issue, which is available at wileyonlinelibrary.com.]

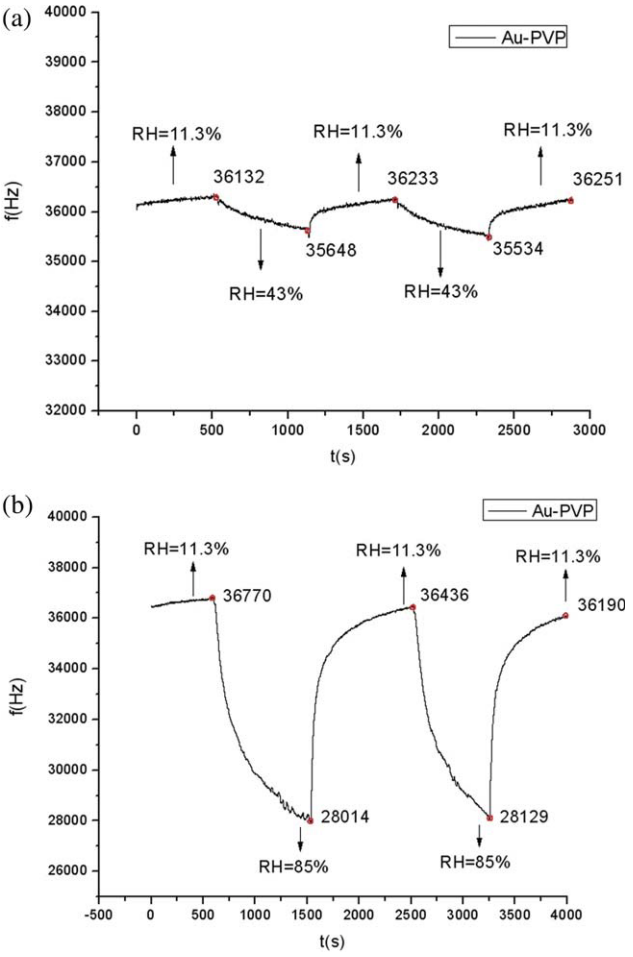

Figure 7 Frequency response curve of the Au–PVP nanocomposites under humidity cycling of (a) 11.3–43–11.3 and (b) 11.3–85–11.3% RH. [Color figure can be viewed in the online issue, which is available at wileyonlinelibrary.com.]

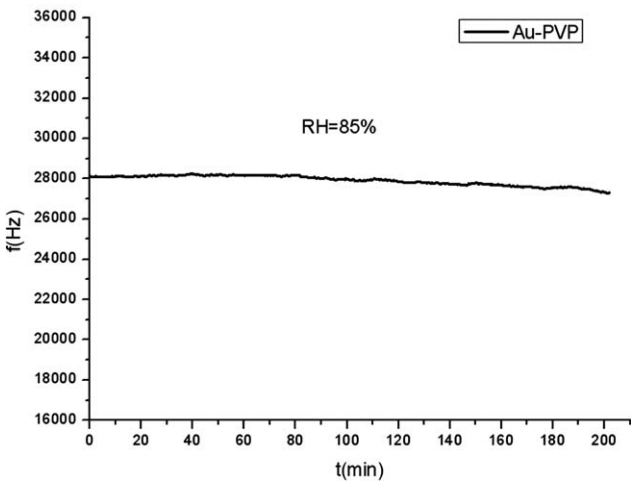

Figure 8 Short-term stability test results of the Au–PVP nanocomposites. t represents the testing time.

in the frequency from the initial humidity stage to the final humidity stage. The response time of the Au–PVP nanocomposites was extracted from the frequency response curves and is shown in Table I. The response time was about 2 or 1 min for increasing or decreasing RH, respectively.

The hysteresis properties of the Au–PVP nanocomposites were first tested in the humidity range from 11.3 to 93% RH, the ascending direction, and then from 93 to 11.3% RH, the descending direction. As shown in Figure 9, the solid curve is the forward direction test, whereas the dashed one is the reverse direction of the hysteresis test. From the humidity cycle of low-to-high and high-to-low steps, one can see that the differences between the ascending and descending curves were very small. The maximum hysteresis rate (E_{max}) was 2.6%, which indicated that the nanocomposites had good frequency reproducibility and low hysteresis:

$$E_{max} = \Delta m / Y_{FS} \times 100\%$$

where Δm is the maximum hysteresis error and Y_{FS} is the full-scale output.

TABLE I
Humidity Response Time of the Au–PVP Nanocomposites Under Different Humidity Levels

RH ascending (%)	Response time (s)	RH descending (%)	Response time (s)
11.3→23	130	23→11.3	88
11.3→43	127	43→11.3	85
11.3→57	108	57→11.3	69
11.3→68	123	68→11.3	56
11.3→75	126	75→11.3	86
11.3→85	130	85→11.3	75
11.3→93	115	93→11.3	68

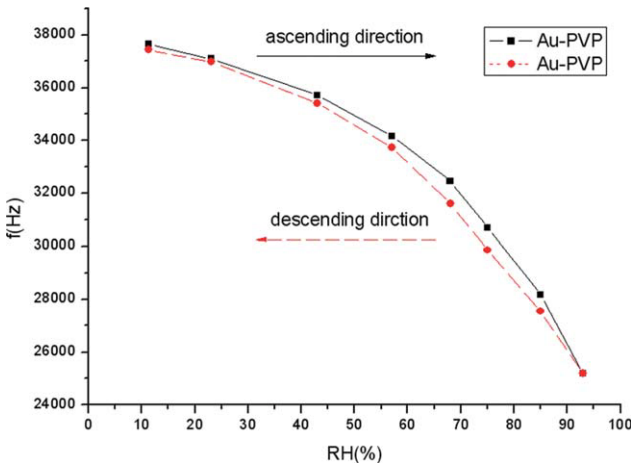

Figure 9 Hysteresis characteristic curve of the Au–PVP nanocomposites. [Color figure can be viewed in the online issue, which is available at wileyonlinelibrary.com.]

CONCLUSIONS

In this study, Au–PVP core–shell nanocomposites were synthesized successfully and applied to capacitive-type humidity sensors as sensing materials. The humidity-sensing properties of the Au–PVP nanocomposites were investigated by the capacitance–frequency conversion circuit. Our study indicated that the Au–PVP nanocomposites showed good performance in most parameters, such as humidity sensitivity, repeatability, stability, response time, and hysteresis properties. Therefore, this material had a good scope for being developed as a capacitive-type humidity sensor for the entire range of humidity.

References

1. Yan, W.; Feng, X. M.; Chen, X. J.; Hou, W. H.; Zhu, J. J. Biosens Bioelectron 2008, 23, 925.
2. Zhang, X. N.; Geng, P.; Liu, H. J.; Teng, Y. Q.; Zhang, W. Biosens Bioelectron 2009, 24, 2155.
3. Yang, Y.; Nogami, M. Sci Technol Adv Mater 2005, 1, 71.
4. Suresh Raj, A. M. E.; Magdalane, C. M.; Nagaraja, K. S. Phys Status Solidi A 2002, 191, 230.
5. Makhlouf, S. A.; Khalil, K. M. S. Solid State Ionics 2003, 164, 97.
6. Chen, T. H.; Xu, P.; Luo, Y. Y.; Jiang, L.; Dan, Y.; Zhang, L.; Zhao, K. J Appl Polym Sci 2009, 114, 496.
7. Chen, D.; Liu, S.; Li, J. J.; Zhao, N. Q. J Alloys Compd 2009, 475, 494.
8. Shan, J.; Tenhu, H. Chem Commun 2007, 44, 4580.
9. Fuke, M. V.; Adhyapak, P. V.; Mulik, U. P.; Amalnerkar, D. P.; Aiyer, R. C. Talanta 2009, 78, 590.
10. Fens, G. Nature: Phys Sci 1973, 241, 20.
11. Burst, M.; Walker, M.; Bethell, D.; Schiffrin, D. J.; Whyman, R. Macromolecules 2009, 42, 2958.
12. Jiang, L.; Guan, J.; Zhao, L. L.; Yang, W. S. Colloids Surf A 2009, 346, 216.
13. Tsai, C. Y.; Chang, T. L.; Chen, C. C.; Ko, F. H.; Chen, P. H. Microelectron Eng 2005, 78–79, 546.
14. Tripathy, P.; Mishra, A.; Ram, S. Mater Chem Phys 2007, 106, 379.
15. Thorp, J. M. J Phys Chem 1962, 66, 1086.
16. Kumar, M.; Sekhon, S. S. Eur Polym J 2002, 38, 1297.
17. Kobayashi, Y.; Kosuge, A.; Konno, M. Appl Surf Sci 2008, 255, 2723.
18. Weast, R. C. CRC Handbook of Chemistry and Physics; CRC: Boca Raton, FL, 1982.
19. Yang, B.; Aksak, B.; Lin, Q.; Sitti, M. Sens Actuators B 2006, 114, 254.